

Anatomy of neck configuration in fission decay

S.K. Patra¹, R. K. Choudhury² and L. Satpathy¹

¹Institute of Physics, Sachivalaya Marg, Bhubaneswar 751005, India

⁴Bhaba Atomic Research Centre, Mumbai

Abstract.

The anatomy of neck configuration in the fission decay of Uranium and Thorium isotopes is investigated in a microscopic study using Relativistic mean field theory. The study includes ^{236}U and ^{232}Th in the valley of stability and exotic neutron rich isotopes ^{250}U , ^{256}U , ^{260}U , ^{240}Th , ^{250}Th , ^{256}Th likely to play important role in the r-process nucleosynthesis in stellar evolution. Following the static fission path, the neck configurations are generated and their composition in terms of the number of neutrons and protons are obtained showing the progressive rise in the neutron component with the increase of mass number. Strong correlation between the neutron multiplicity in the fission decay and the number of neutrons in the neck is seen. The maximum neutron-proton ratio is about 5 for ^{260}U and ^{256}Th suggestive of the break down of liquid-drop picture and inhibition of the fission decay in still heavier isotopes. Neck as precursor of a new mode of fission decay like multi-fragmentation fission may also be inferred from this study.

PACS: 24.75.+i, 25.85.-w, 21.10.Dr, 21.60.Jz

Keywords: Nuclear Fission, neck structure, scission point, relativistic mean field formalism

1. Introduction

Although the phenomenon of nuclear fission has been discovered since about sixty years back, many crucial facets of this process are still not understood at fundamental level, warranting further exploration of its dynamics. This is more so when viewed from the microscopic theoretical point of view. From the early days, the two goals of nuclear theory were to explain the fission phenomena and the working of the nuclear independent-particle shell model in terms of the nuclear Hamiltonian involving nucleon-nucleon interaction. Although the later goal is more or less reached, the former is still languishing in the mid way. The general methods followed in such studies are nonrelativistic selfconsistent mean-field theories like Hartree-Fock (HF), Hartree-Fock Bogolybu (HFB), Hartree-BCS etc. and their derivatives. These theories are more suitable for finding the static fission path [1, 2, 3, 4], however they can be used to exhaustively map the entire potential energy landscape spanned by relevant degrees of freedom revealing main features of fission dynamics. In an improved microscopic calculation fission is described by performing the time evolution of a single determinantal

many-body wave function in the framework of time-dependent Hartree-Fock (TDHF) theory [5]. Such attempts imposing restrictive constraints, have been done with limited success. The proper microscopic theory for fission is the adiabatic time-dependent Hartree-Fock (ATDHF) developed by Villars and others [6, 7] to deal with effectively the large amplitude slow evolution of the nuclear shape in this process. In this theory, one can calculate the dynamic fission path without computing the entire energy landscape. However the practical application to date has been rather very limited [7] primarily because of its complexity. In a recent development a new microscope approach based on Time Dependent Generator Coordinate Method (TDGCM) has been proposed [8] using solutions of Hartree-Fock Bogolyubov mean field theory and Gaussian overlap approximation. The theory is equipped to describe the time-dependent evolution of the fission process whose initial applications look promising. The most popular and widely used microscopic-macroscopic method [9] is semi-microscopic in nature, consisting of a liquid drop part and a shell correction part for the total energy of the nucleus. The exploration of the multidimensional energy landscape has been quite successful in this method [10]. In such approach, specifically introducing neck degree of freedom and using two-centre microscopic potential to favour the formation of two fragments, studies [11, 12] have been made to investigate specific questions like how neck influences the fission paths and emission of scission neutrons etc. Here we have entertained a specific objective of studying the neck configuration following the static fission path at a fundamental level using microscopic nuclear many-body Hamiltonian, with the hope of unraveling some core features of fission dynamics, for which we have adopted the relativistic mean field (RMF) theory.

The critical feature of the fission phenomena is the multiplicity of neutron emitted in this process, which plays key role in the chain reaction leading to energy generation. In the commonly used thermal fission of ^{235}U , the multiplicity of the neutron is 2.5, emitted by the two fragments in the post scission stage after they are accelerated by the mutual Coulomb repulsion. In this reaction, the neck is believed to be neutron rich as the neutron emission from this region have been observed [13, 14] to be more than that of the α - particle and the proton emission. Experimentally it may not be possible to ascertain the true composition of the neck, which has potential to reveal important aspects of the mechanism of fission dynamics. It will be truly rewarding if it would be possible to generate theoretically the neck, and find neutron-proton composition in a quantitative manner. Such study will open up the possibility for understanding the fission of highly neutron-rich actinide nuclei, likely to be synthesised in the RIB facilities under construction in many laboratories around the world [15]. How does such a nucleus undergo fission is a very pertinent question with potential to be an exciting theme of research in future. The composition of neck in the fission of such nuclei may contain informations regarding new physics. Various mass formulae have predicted that Uranium isotope with mass number as high as 270 and even more upto 290 to be particle stable. The progressive production of such nuclei in the r-process of nuclear synthesis in stellar evolution is more real than speculative. The continued synthesis of successively

heavier isotopes of an element by neutron capture in this process is finally terminated by fission. In an earlier study [16], we have identified a valley where Uranium and Thorium isotopes with neutron number in the range $N=154-172$ to be thermally fissile, a reflection of the close shell structure of $N=162 \sim 164$ predicted in numerous calculations over the years. Therefore in our calculation we have included, besides the two well known stable nuclei ^{232}Th and ^{236}U the exotic nuclei ^{250}U , ^{256}U , ^{260}U , ^{240}Th , ^{250}Th and ^{256}Th far from this stability valley.

A more exciting impetus to study the above nuclei originates from the expectation to find new phenomena in this virgin nuclear territory of high neutron to proton ratio, widely speculated to be manifested. The maximum neutron to proton ratio of neck found to be about 5 for the heaviest isotopes ^{260}U and ^{256}Th considered here. The heavier isotopes than these ones will not support neck suggestive of the break down of the liquid drop picture. Our recent study [16] of ^{250}U gives strong evidence of new mode of fission decay termed as 'multifragmentation fission' in which 2.5 neutrons are emitted at scission along with the two fragments, in addition to the usual 2.5 prompt neutrons in the post scission stage. The present study of the composition of the neck configuration has the potential to be a precursor of such a phenomenon and even of some more exotic ones. In Sec.2, we present an outline of our scheme of calculation in the RMF theory. The calculations and results are given in Sec.3, and discussions in Sec.4. Sec. 5 contains the conclusion.

2. Scheme of calculation in RMF theory

A brief sketch of the RMF theory [17, 18] is outlined here for completeness. The relativistic Lagrangian density for a nucleon-meson many-body system is given by

$$\begin{aligned}
 \mathcal{L} = & \bar{\psi}_i \{ i\gamma^\mu \partial_\mu - M \} \psi_i + \frac{1}{2} \partial^\mu \sigma \partial_\mu \sigma - \frac{1}{2} m_\sigma^2 \sigma^2 \\
 & - \frac{1}{3} g_2 \sigma^3 - \frac{1}{4} g_3 \sigma^4 - g_s \bar{\psi}_i \psi_i \sigma - \frac{1}{4} \Omega^{\mu\nu} \Omega_{\mu\nu} \\
 & + \frac{1}{2} m_w^2 V^\mu V_\mu + \frac{1}{4} c_3 (V_\mu V^\mu)^2 - g_w \bar{\psi}_i \gamma^\mu \psi_i V_\mu \\
 & - \frac{1}{4} \vec{B}^{\mu\nu} \cdot \vec{B}_{\mu\nu} + \frac{1}{2} m_\rho^2 \vec{R}^\mu \cdot \vec{R}_\mu - g_\rho \bar{\psi}_i \gamma^\mu \vec{\tau} \psi_i \cdot \vec{R}^\mu \\
 & - \frac{1}{4} F^{\mu\nu} F_{\mu\nu} - e \bar{\psi}_i \gamma^\mu \frac{(1 - \tau_{3i})}{2} \psi_i A_\mu.
 \end{aligned} \tag{1}$$

From this Lagrangian we obtain the field equations for the nucleons and mesons. These equations are solved by expanding the upper and lower components of the Dirac spinors and the boson fields in an axially deformed harmonic oscillator basis. The set of coupled equations is solved numerically by a self-consistent iteration method. Here we get bosonic equation for σ , ω and ρ mesons and Dirac equation for the nucleons. The σ -field gives the attractive and the ω - field gives the repulsive component of the nuclear potential. However, the ρ meson field takes care of the proton-neutron asymmetric

energy. In our calculation, the constant gap BCS pairing is used to add the pairing effects for open shell nuclei. The centre-of-mass motion (c.m.) energy correction is estimated by the usual harmonic oscillator formula $E_{c.m.} = \frac{3}{4}(41A^{-1/3})$.

In the present investigation, we have carried out study microscopically in the nonlinear RMF theory of Boguta and Bodmer [19], an extended version of Walecka [17] theory. We have adopted the NL3 [20] interactions. The NL3 interaction has been widely used in recent years in the calculation of varieties of nuclear properties like binding energy, *rms* radii and giant resonances etc. and have been accepted to be very successful. Here we have studied the stability of our result for each nucleus by varying the number of harmonic oscillator shells used in the basis between $N_F = N_B = 12$ to 28. The quadrupole deformation parameter β_2 is evaluated from the resulting proton and neutron quadrupole moments, as $Q = Q_n + Q_p = \sqrt{\frac{16\pi}{5}}(\frac{3}{4\pi}AR^2\beta_2)$. The *rms* matter radius is defined as $\langle r_m^2 \rangle = \frac{1}{A} \int \rho(r_\perp, z)r^2 d\tau$; here A is the mass number, and $\rho(r_\perp, z)$ is the deformed density. As outputs, we obtain different potentials, densities, single-particle energy levels, radii, quadrupole deformations and the binding energies. For a given nucleus, the maximum binding energy corresponds to the ground-state and other solutions are obtained as various excited intrinsic states, provided the nucleus does not under go fission. The density distribution of nucleons plays the prominent role in the study of the internal structure of a nucleus. When the deformation of a nucleus is varied, the density distribution $\rho(r_\perp, z)$ inside the nucleus also varies. For example, the $\rho(r_\perp, z)$ for a spherical nucleus is symmetrical in (r_\perp, z) -plane. However, it is highly asymmetric for a largely deformed nucleus. Knowing the density distribution of the spherical or (oblate/ prolate) deformed configuration, we can calculate the number of nucleons for each configuration, defined as

$$N = \int \int \rho_n(r_\perp, z) d\tau, \tag{2}$$

$$Z = \int \int \rho_p(r_\perp, z) d\tau, \tag{3}$$

where ρ_n and ρ_p are the neutron and proton density of the nucleus, and the the total density $\rho = \rho_n + \rho_p$. We have obtained the static fission path by calculating the potential energy surface (PES) using the above RMF formalism in a constrained calculation [21, 22, 23, 24], i.e., instead of minimizing the H_0 , we have minimized $H' = H_0 - \lambda Q_2$, with λ as a Lagrange multiplier and Q_2 , the quadrupole moment. Thus, we get the solution at a given quadrupole deformation and then obtain the energy using the H_0 .

3. Calculation and Result

The fission process has been traditionally visualized in liquid-drop picture, where the nuclear surface is expressed in terms of collective deformation parameters characterized by several multipole shapes with quadrupole deformation playing the most important role. Classically, it corresponds to slow movement of the nucleus from the ground state

equilibrium shape along a slowly rising valley path in the energy landscape spanned by the deformation variables. It reaches the barrier top (saddle point), and then slides down on the outer surface of the barrier and acquires a highly elongated shape culminating in a narrow neck which finally splits into two fragment nuclei. Quantum mechanically this path upto the scission point defines a potential barrier, which can be used for calculating the transmission coefficient to obtain the fission probability. It is this path normally called static fission path, which we intend to calculate here. Since quadrupole deformation plays the predominant role, we have chosen it in our calculation and ignored the other deformation coordinates for simplicity, being guided by the goal for studying the anatomy of neck configurations exhaustively.

It is worth pointing out that a nucleus undergoes binary fission in various modes with different probabilities. The neck configuration in each mode is likely to be different from those of the other modes depending upon the respective pairs of fragment nuclei. Therefore, the necks for the symmetric and asymmetric configurations will be different, and so also their scission points.

In our calculations we have imposed time reversal symmetry, reflection symmetry across XY plane and rotational symmetry about the Z-direction, i.e, the fission direction. So naturally we arrive at symmetric fission. Möller et al.[10] have found two different paths leading to symmetric and asymmetric fission in their study in five-dimensional deformation space. We did not get solution for the configuration with two separated fragments in our calculations, which may be attributed to the limitation of the numerical computation/mean field theory.

In Table 1, we have presented our results on the energy, deformation, rms radius of the ground-state and neck configuration of the two known nuclei ^{236}U and ^{232}Th in the valley of stability and the six exotic neutron-rich nuclei ^{250}U , ^{256}U , ^{260}U , ^{240}Th , ^{250}Th and ^{256}Th away from it. To begin with it will be interesting and reassuring to see how well the ground-state properties of these two known nuclei are reproduced in our calculation. The experimental values of these properties are presented in parenthesis below the corresponding theoretical values in the same table. It can be seen that the ground-state energy, the deformation and rms radius of these two nuclei compare remarkably well with experiment. This reassures us about the goodness of the interaction and the suitability of the RMF theory for this study.

In the next step, we calculate the static fission-path and examine if the general fission properties like the barrier and its double-humped characteristics are reproduced. Although we have performed static path calculation for all the eight nuclei we present here only the results of the widely studied nucleus ^{236}U , and one of the exotic nuclei, i.e., ^{250}U . In Fig. 1 we have plotted the energy as a function of the deformation parameter for these two nuclei. From the figure, it can be seen that the fission barrier for ^{236}U comes out to be 6.95 MeV comparable to the experimental value of 5.75 MeV [28]. The fission barrier of 4.05 MeV in case of ^{250}U obtained in our calculation, is expectedly lower than that of ^{236}U which agrees with the Howard-Möller value of 4.3 MeV. The double-humped fission barriers in both cases have been reproduced. These results are

Table 1. The RMF(NL3) results for binding energy BE, the quadrupole deformation parameter β_2 and *rms* radius for both the ground and neck configurations for ^{236}U , ^{250}U , ^{256}U , ^{260}U , ^{232}Th , ^{240}Th , ^{250}Th and ^{256}Th . The experimental values wherever known are given in parenthesis.

Nucleus	State	β_2	$r_c(fm)$	BE (MeV)
^{236}U	Ground	0.26 (0.28[25])	5.86 (5.84 [27])	1790.5 (1790.4 [26])
	Neck	6.04	12.14	1808.5
^{250}U	Ground	0.26	5.82	1856.5
	Neck	5.52	11.91	1890.7
^{256}U	Ground	0.18	5.97	1880.6
	Neck	5.41	11.78	1914.7
^{260}U	Ground	0.15	5.99	1895.3
	Neck	5.37	11.74	1923.9
^{232}Th	Ground	0.26 (0.26[25])	5.83 (5.71 [27])	1767.1 (1766.7[26])
	Neck	5.79	11.88	1789.0
^{240}Th	Ground	0.26	5.90	1806.3
	Neck	5.52	11.66	1825.2
^{250}Th	Ground	0.22	5.93	1846.3
	Neck	5.45	11.84	1872.2
^{256}Th	Ground	0.16	5.96	1868.8
	Neck	5.31	11.72	1891.5

indeed very satisfying. We have followed the density profile of the evolving fragments along with the neck, to findout a criterion for the delineation of the latter. We observe in general that, this profile has the form of a Fermi distribution in the fragment region as expected, with the tail part attaining a constant value. We have chosen the criterion that when the density falls to 15% of the central density and remains constant along the Z-coordinate, then neck is assumed to originate which merges on the other fragment with the endpoint being defined with similar criterion.

We have presented in Fig. 2, the matter density distributions of some typical configurations these two nuclei acquire, in their static fission-path right upto the neck configuration. It is satisfying to see well defined dumbbell shape of neck reproduced in RMF study as solution of microscopic nuclear many-body Hamiltonian, in agreement with age-old picture of fission process envisioned in classical liquid drop model. The physical characteristics of the necks of these systems emerging from this study will be discussed along with the other six nuclei a posteriori. In a recent microscopic study using constrained HFB method with Gogny interaction Dubray et al [2], obtained very elongated shape without clear-cut neck before the scission in Th and Fm isotopes, and found that these fissioning systems energetically favoured splitting into two separate fragments rather than develop an elongated shape with a neck. Banneau [29] obtained similar results for Fm isotope in his study using Skyrme-Hartree-Fock-BCS model.

Since our objective has been to critically study the neck configurations, we have presented their matter density distributions in Figures 3 and 4, obtained in our calculation of the four Uranium isotopes and four Thorium isotopes respectively. As noted above, the energies, rms radii and deformations of the neck configuration and the ground-states for all the eight nuclei can be seen in Table 1. The five nuclei ^{236}U , ^{250}U , ^{232}Th , ^{240}Th and ^{250}Th have similar ground-state deformation with β_2 values around 0.26. The remaining three nuclei ^{256}U , ^{260}U and ^{256}Th have significantly lower β_2 values around 0.16 which may be a reflection of the proximity of their neutron numbers to shell closure $N=164$. The ground-state rms charge radii of all the nuclei are around 6 fm; the corresponding radii of the neck configurations are nearly twice being around 12 fm which are very much expected. As can be seen in the Table I, the neck configurations lie around 20 MeV below the respective ground-states in conformity with expectation and in agreement with our general notion of fission dynamics. From the matter density distributions in Figs. 3 and 4, it is clear that all the cases are of symmetric fission. To see how far our neck configuration in ^{236}U conforms to reality, we have calculated the kinetic energy that will be generated if it breaks into two fragments. It comes out to be 139 MeV which may be compared with the most probable value of 155 MeV observed in low energy fission of ^{236}U corresponding to asymmetric mass split.

4. Characteristics of neck

4.1. Density and N/Z composition

Our calculation yields the matter density ρ , the neutron density ρ_n and the proton density ρ_p at every point in the body of system [30]. The total number of neutrons N_{neck} and the number of protons Z_{neck} contained in the neck, are obtained by integrating the corresponding densities over its physical dimension of the neck using Eq. (1). The results are presented in Table 2. We have also presented the mean densities $\bar{\rho}_n = \int \rho_n d\tau / d\tau$, $\bar{\rho}_p = \int \rho_p d\tau / d\tau$, of the necks in the same. As expected the $\bar{\rho}_p$ for both the elements remain similar for all their isotopes being around 0.035 fm^{-3} . As for the $\bar{\rho}_n$ for both the systems the values generally increase with the increase of the neutron number of the isotopes. It can be seen that with the increase of the neutron number in the isotope, the neutron to proton density ratio $\bar{\rho}_n / \bar{\rho}_p$ increases generally, as expected. For U-isotopes, the ratio has increased from 1.70 for ^{236}U to 3.0 for ^{260}U . The corresponding number is 1.51 for ^{232}Th to 2.73 for ^{256}Th .

We have estimated the number of neutrons and protons contained in the neck by using Eq. (1), which are presented in Table 2. As we move from ^{236}U to ^{260}U , the number of neck neutrons increases from 2.42 to 5.11 and the proton number almost does not change. Similar trend is seen for Th isotopes with rise from 1.71 for ^{232}Th to 3.78 for ^{256}Th . It may be observed that the value of N_{neck}/Z_{neck} is some what different from that of $\bar{\rho}_n/\bar{\rho}_z$ in Table 2, because the effective volumes for neutron and proton distributions are different, the latter being somewhat smaller than the former due to its

Table 2. The Characteristics of neck configuration. The average neutron and proton densities $\bar{\rho}_n(fm^{-3})$, and $\bar{\rho}_p(fm^{-3})$ and their ratios $\bar{\rho}_n/\bar{\rho}_p$, number of neutron and proton N_{neck} and Z_{neck} contained in the neck, rms charge radius $r_c^{nk}(fm)$, length of the neck $L_n(fm)$, the centre to centre distance $l_{cc}(fm)$ and tip to tip distance of the neck $L_t(fm)$ are presented.

Nucleus	$\bar{\rho}_n$	$\bar{\rho}_p$	$\bar{\rho}_n/\bar{\rho}_p$	Z_{neck}	N_{neck}	$\frac{N_{neck}}{Z_{neck}}$	r_c^{nk}	L_n	l_{cc}	L_t
^{236}U	0.058	0.034	1.70	0.95	2.42	2.54	12.14	6.28	21.88	37.48
^{250}U	0.074	0.031	2.37	0.86	3.23	3.75	11.91	5.82	21.56	37.30
^{256}U	0.085	0.031	2.74	0.82	3.77	4.59	11.78	5.46	21.30	37.14
^{260}U	0.093	0.031	3.00	1.03	5.11	4.96	11.74	4.29	21.18	37.07
^{232}Th	0.062	0.041	1.51	0.66	1.71	2.59	11.88	5.18	21.80	38.42
^{240}Th	0.071	0.042	1.69	0.69	2.47	3.57	11.86	4.76	21.44	38.12
^{250}Th	0.081	0.034	2.38	0.62	2.94	4.74	11.82	4.68	21.10	37.52
^{256}Th	0.090	0.033	2.73	0.68	3.78	5.55	11.72	4.52	20.74	36.96

considerable low number. This high neutron-proton ratio is a precursor of a new mode of fission decay which will be discussed a posteriori.

The maximum ratio of neutron to proton in the neck found by us is around 5 for the heaviest isotopes ^{260}U and ^{256}Th considered by us. Quasi-bound/resonance for 5H , 6H have been known; no such states for heavier isotope of hydrogen above 6H have been observed. Neck can be considered a quasi-bound transient state. Thus our finding of the maximum N/Z ratio in the neck correlates with these transient states observed in nature. The nuclear matter inhabiting the neck region in the heaviest isotope ^{260}U considered here has the neutron to proton ratio about 5:1 which corresponds to 6H system. Since 7H system is the likely limiting surviving resonance with half-life of 23×10^{-24} sec. only and resonances of still heavier hydrogen isotopes are unlikely to be found in nature, it is reasonable to conclude that such nuclear liquid is not viable. Therefore neck formation in somewhat heavier than ^{260}U isotope requiring such nuclear liquid with higher neutron to proton ratio than 6:1 will be unsustainable, which signals break-down of the usual liquid-drop picture of the fission process visualized so far. Since neck can not be formed as the nuclear liquid-drop picture breaks down and so fission will be inhibited in such heavy neutron-rich isotopes. This effect is also manifested in progressive shrinking of the elongation of the neck with rise of neutron number in heavier isotopes (see Table 2) which may eventually disappear with increase of mass. Thus the predominant mode of decay of such nuclei will be β -decay. The situation seems parallel to the case of superheavy element in the valley of stability where α -decay becomes more preferred mode of decay over fission.

4.2. Size and Extension

How far the nucleus extends in its neck configuration compared to its size in its ground-state ? In Table 2, we have presented the charge radius of the neck configuration r_c^{nk} ,

length of the neck L_n , i.e. the distance between the two facing surfaces connected by the neck, l_{cc} the distance between the centre of the two fragments and L_t the distance between the two tips which is a measure of the extension. The charge radii of the neck for all the isotopes are around 12 fm (see Table 1). The length of the neck L_n is around 5 fm for the two nuclei ^{236}U and ^{232}Th . The value decreases with the rise of the neutron number reaching 4.29 fm for ^{260}U and 4.52 fm for ^{256}Th . Less elongated neck for heavier isotopes is a reflection of the fact that, decrease of binding energy due to increase of neutron to proton ratio, does not support a longer configuration but a shorter one.

The tip to tip distance L_t is around 37 fm in all the cases. Thus, well defined neck and fairly extended mass distribution in this configuration is evident in all cases. It is indeed interesting to find, very heavy nuclei acquiring such extended dumbbell configuration supported by nucleon-nucleon force. It is useful to recall here that light 4n nuclei like ^{16}O , ^{20}Ne , ^{24}Mg , ^{28}Si etc. exhibit very long physical states with linear α -cluster configuration[31].

4.3. Precursor of a new mode of fission decay

Since neck is the most sensitive part where rupture takes place giving rise to two heavy fission fragments, its composition will play a crucial role in determining the fission dynamics. In widely studied ^{236}U , the decay process is binary; at the instant of the rupture of the neck, each of two protruding parts originating from the rupture of the neck is sucked in by the respective connecting fragments. Then the two fragments move in opposite direction, being repelled by the mutual Coulomb repulsion, and emit 2.5 neutrons in the process of de-excitation to the respective ground-states. The sucking of the half of the neck by a fragment is possible because of the presence of sizable number of protons (as shown in the present calculations) in the neck providing attractive nuclear force. However in the heavier isotopes like ^{250}Th , ^{256}Th , ^{250}U , ^{256}U and ^{260}U the proton components are relatively smaller compared to the neutron components. The likely scenario in such a system is that the triplet-triplet and singlet-singlet components of nucleon-nucleon force which are repulsive in nature become dominant, and therefore sucking in is unlikely to happen, and the ruptured neck may not be able to hold on all the neutrons, and may simultaneously release them along with the production of the two fragments. This will be a new mode of fission decay as mentioned in the introduction known as *multifragmentation fission* proposed earlier by the authors [16]. In such cases, the multiplicity of neutron will consist of two parts: the usual prompt neutrons plus the multifragmentation neutrons generated at the time of scission contributed by the neck. Taking into account the neck neutrons calculated above, and assuming the modest value of 2.5 for prompt neutrons similar to that of ^{236}U , the multiplicities are expected to be more than 4 for ^{250}U , ^{256}U , ^{260}U , ^{250}Th and ^{256}Th . This prediction will get strong support from the probability of fragment mass-yield as shown below.

The important driving force for the decay of a nucleus is the Q-value of the reaction. The probability of fragment mass-yield in fission process is directly related to the Q-value

and temperature at the scission point. We therefore calculate the Q-value systematics of the fission of the nucleus (A, Z) decaying to (A_1, Z_1) and (A_2, Z_2) defined as:

$$Q_{fiss.}(A, Z) = BE(A_1, Z_1) + BE(A_2, Z_2) - BE(A, Z) \quad (4)$$

To avoid clumsiness we have plotted the Q-values in Fig. 5 for the 6 isotopes $^{236,250,260}\text{U}$ and $^{232,250,256}\text{Th}$ for the possible binary decays $(A, Z) = (A_1, Z_1) + (A_2, Z_2)$ taking even values of Z_1 in the range 39 to 46, with varying A_1 , the complementary fragment (A_2, Z_2) being thereby fixed. Since the yield falls rapidly with the decrease of the Q-value for an element, the values lying above 90% of the highest value are only relevant.

For the present study we have used the masses predicted in the finite range droplet model (FRDM) [28] and infinite nuclear mass model (INM) [32]. We have chosen the latter mass model for its unique success in describing the saturation properties [33] of INM, shell quenching [34] in the large neutron $N=82, 126$ shells and its long range predictive ability especially in the neutron rich side. For each element the two vertical lines in the figures refer to the drip-lines predicted in the two mass models which agree within $3 \sim 5$ neutrons. Except for the three isotopes ^{232}Th , ^{236}U and ^{240}Th in the valley of stability, in the remaining five cases, the drip-lines fall within the Q-value distributions with a few touching the outer fringes. To avoid clumsiness we depict in Fig. 5 the cases of 6 isotopes only. All the isotopes lying to the right of the drip-line will be unstable against the instantaneous release of the neutrons from the fragments at the scission. In the usual fission process of ^{236}U , neutrons are emitted from the fragments after they are accelerated. But the five cases of heavy isotopes ^{250}U , ^{256}U , ^{260}U , ^{250}Th and ^{256}Th a certain number of neutrons will be simultaneously emitted along with the two heavy fragments. It will be interesting to see if the number of multifragmentation neutrons which can be estimated taking the drip-line nucleus as the last surviving fragment, and compare the same with the number of neutrons in the neck. It is expected that there will be a correlation between the number of neck neutrons and the multifragmentation neutrons which will be emitted by the fragments being populated beyond drip-line at scission. It is reasonable to suppose the excess of neutrons beyond the drip-line are likely to be lodged in the neck. From the Q-value distributions of ^{260}U it can be seen that about 5 multifragmentation neutrons will be emitted (ignoring the one or two units of neutron difference between predictions of the two mass formulae) in most of the decay modes which agree with the neutron number in the neck (see Table 2). In the case of ^{256}Th the corresponding number is about 4 neutrons. Thus in the fission process of exotic neutron-rich isotopes, the picture emerges that, the neutrons beyond the drip-line contained in the fission fragments are likely to take part in the neck formation. It is interesting to see that there is a qualitative agreement. It must be recognised that these scission neutrons are the extra neutrons in addition to the normal multiplicity of neutrons emitted from the fragments. Thus the total multiplicity will be more than doubled. It will have serious implication in the chain reaction, the key process for energy generation in fission. We would like to emphasize that although at the moment this new

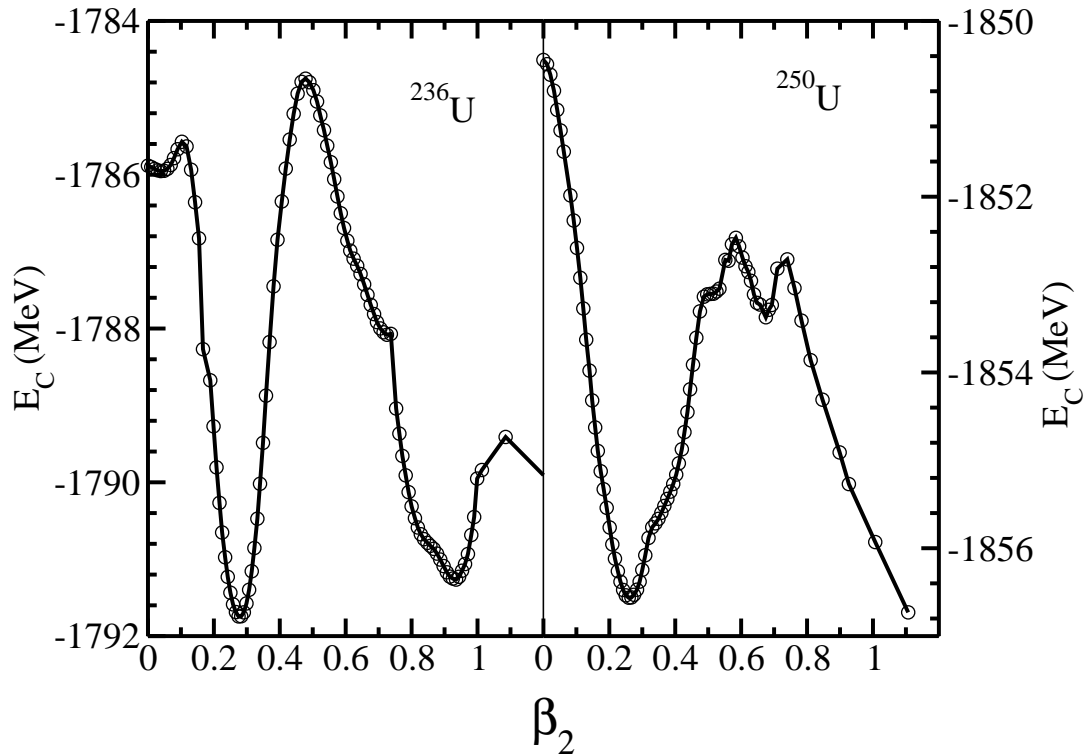


Figure 1. The energy curves of ^{236}U and ^{250}U as a function of the deformation parameter β_2 obtained in the Relativistic mean field formalism with NL3 parameter set.

decay mode of fission may not be realised in the laboratory, it is very likely occurring in the r-process nucleosynthesis of terrestrial evolution.

5. Summary and Conclusions

We have attempted to understand the mechanism of fission decay by following the static fission path, and concentrating on the ultimate shape of the nucleus it likely to acquire, before the break up, i.e., the neck configuration. This picture envisaged since the very early days of nuclear physics viewing the nucleus to be a classical liquid, is reaffirmed here in a microscopic study carried out in the framework of established nuclear theory employing wellknown many-body nuclear Hamiltonian. The RMF theory which has gained the confidence of nuclear communities as a viable theory has been adopted in the present study. In our calculation, it has been possible to access such highly deformed configuration as neck by using very large basis consisting of as many as 28 oscillator states, while for ground-state 10 or 12 states are adequate. This study has bared the anatomy of neck, revealing rich neutron-proton ratio, which progressively increases with the neutron number in the isotope. We have been able to find out the length of the neck and its neutron-proton composition in term of their numbers. The maximum neutron to proton ratio found by us is 5 which may correlate with the quasi-bound/resonance state of the heaviest hydrogen isotope ^6H known so far. This neck with higher neutron

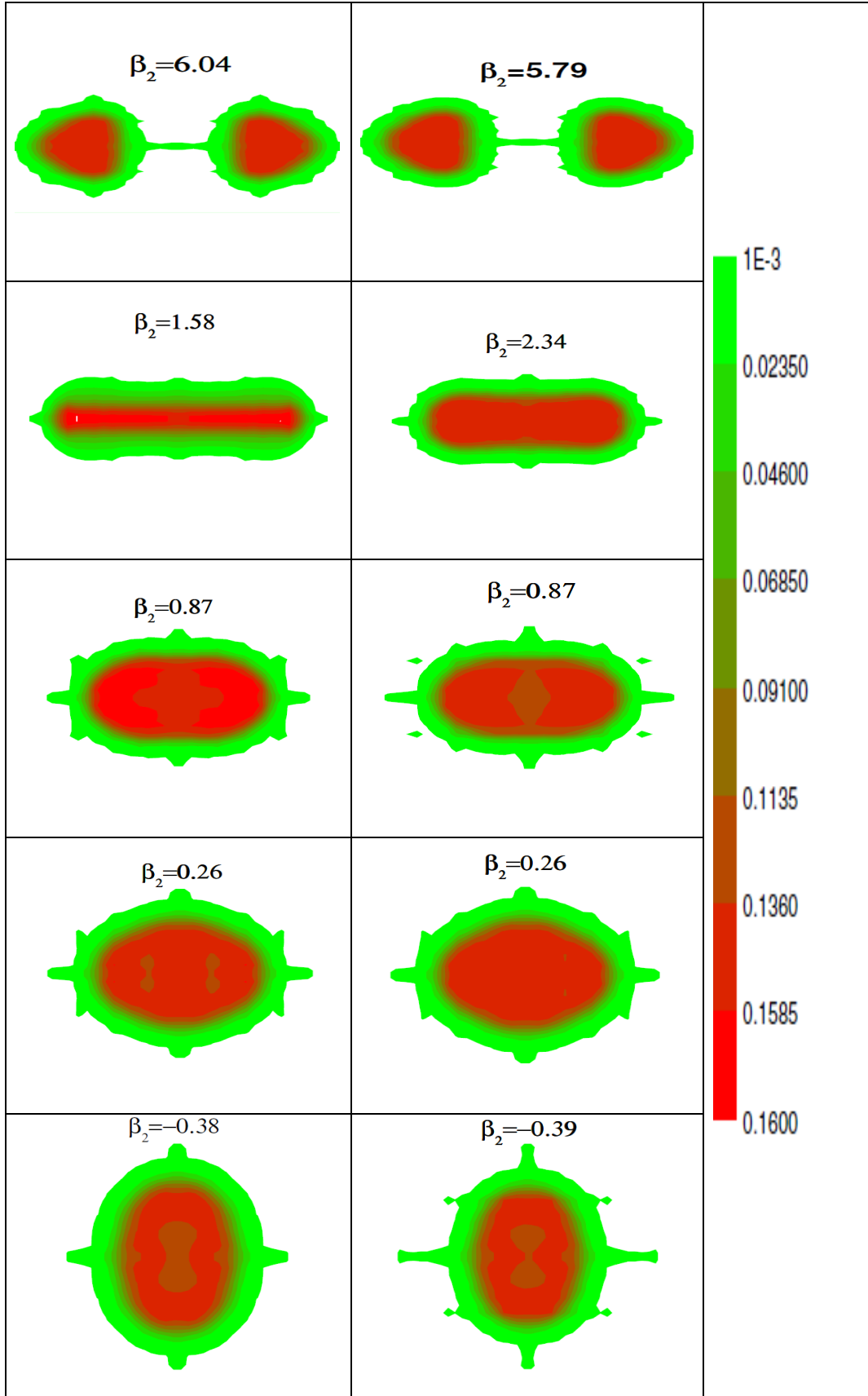


Figure 2. Evolution of neck for the isotopes of Uranium and Thorium. The matter density distributions for different deformation β_2 of ^{236}U and ^{232}Th obtained in the relativistic mean field formalism using NL3 parameter set. The total (neutron+proton) number density $\rho = \rho_n + \rho_p$ in fm^{-3} is shown

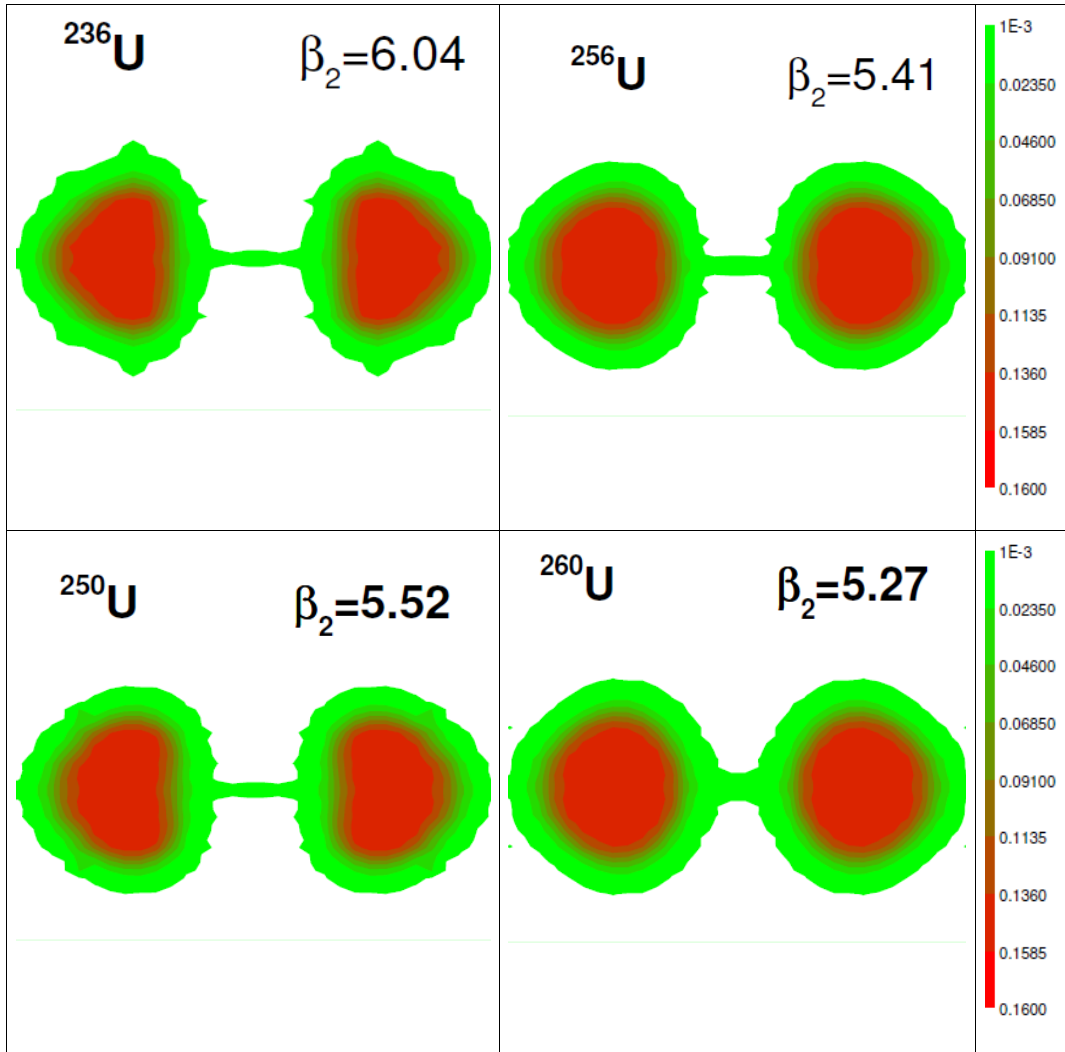


Figure 3. The matter density distributions for the neck structure of Uranium isotopes in a relativistic mean field formalism using NL3 parameter set. The total (neutron+proton) number density $\rho = \rho_n + \rho_p$ in fm^{-3} is shown.

to proton ratio then 6 are not likely to be formed. This suggests that heavier isotopes of Uranium than ^{260}U may undergo fission without formation of neck or more likely fission is inhibited. This may be a new feature of fission to be found in ultra-neutron-rich Uranium isotopes which signals the breakdown of liquid-drop picture.

In our investigation, besides the wellknown actinide nuclei ^{236}U and ^{232}Th in the valley of stability, their highly neutron-rich isotopes ^{250}U , ^{256}U , ^{260}U , ^{240}Th , ^{250}Th , ^{256}Th have been included with the objective of finding the fission properties of such exotic nuclei of relevance in stellar evolution. Some of these nuclei with lower mass number are likely to be synthesised in the RIB facilities. The highly neutron-rich necks found in the calculation in the above exotic nuclei, points out a new mode of fission decay where along with the two heavy fragments some neutrons will be emitted simultaneously at scission. These are extra neutrons in addition to the usual neutron multiplicity emitted

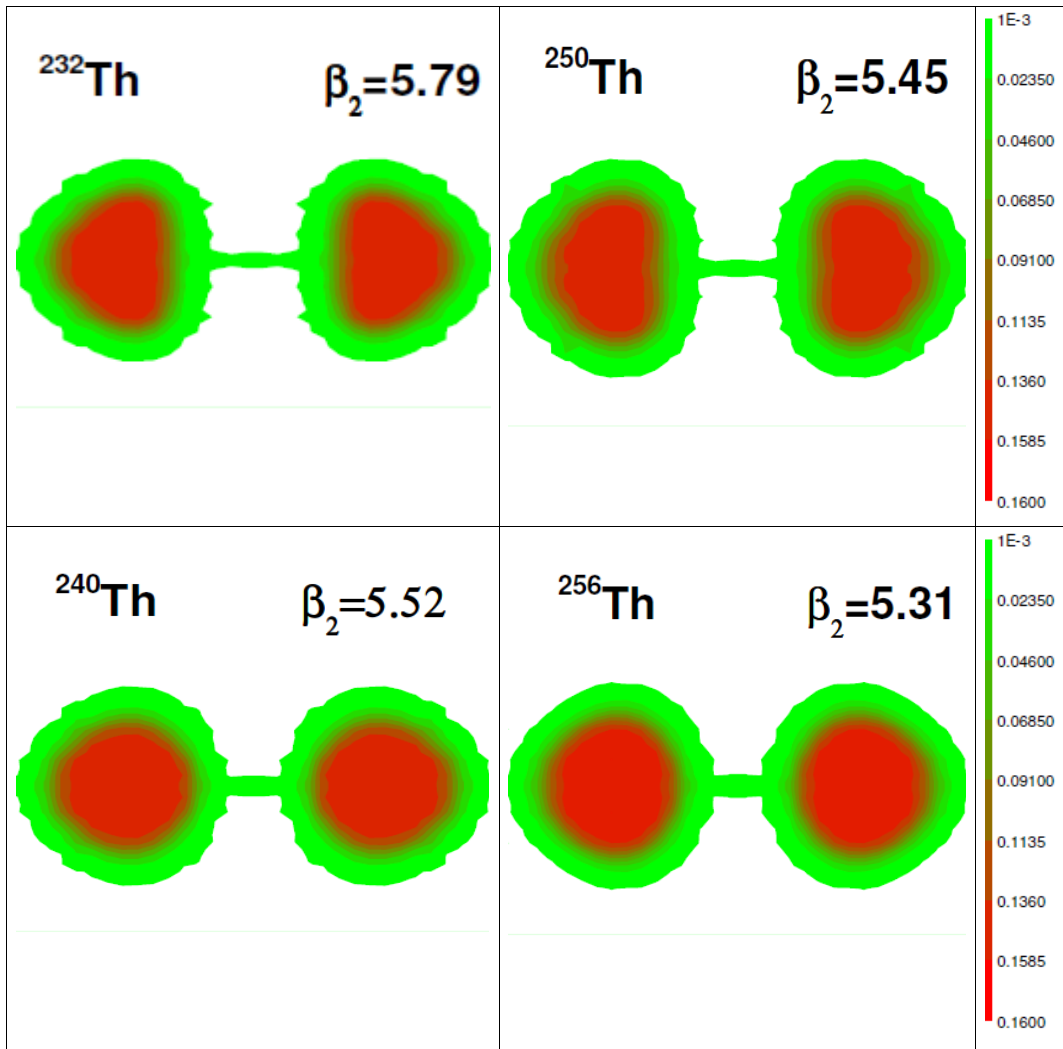


Figure 4. Same as Figure 2, but for Thorium isotopes.

by the two fragments later in the flight. Thus total multiplicity gets more than doubled of the expected usual one. Due to extreme neutron-richness of the neck it can not be sucked into the two fragments at scission, but itself breaks down contributing these neutrons. This inference is supported by our fission mass-yield study carried out using Q-value systematics. It will have serious implication in the energy generation process in the r-process nucleosynthesis in stellar evolution. Whether this process will be of any utility in the laboratory is too premature to speculate at the moment.

6. Acknowledgments

This work is supported in part by Council of Scientific & Industrial Research (No.03 (1060) 06/EMR-II), as well as the Department of Science and Technology, Govt. of India, project No. SR/S2/HEP-16/2005.

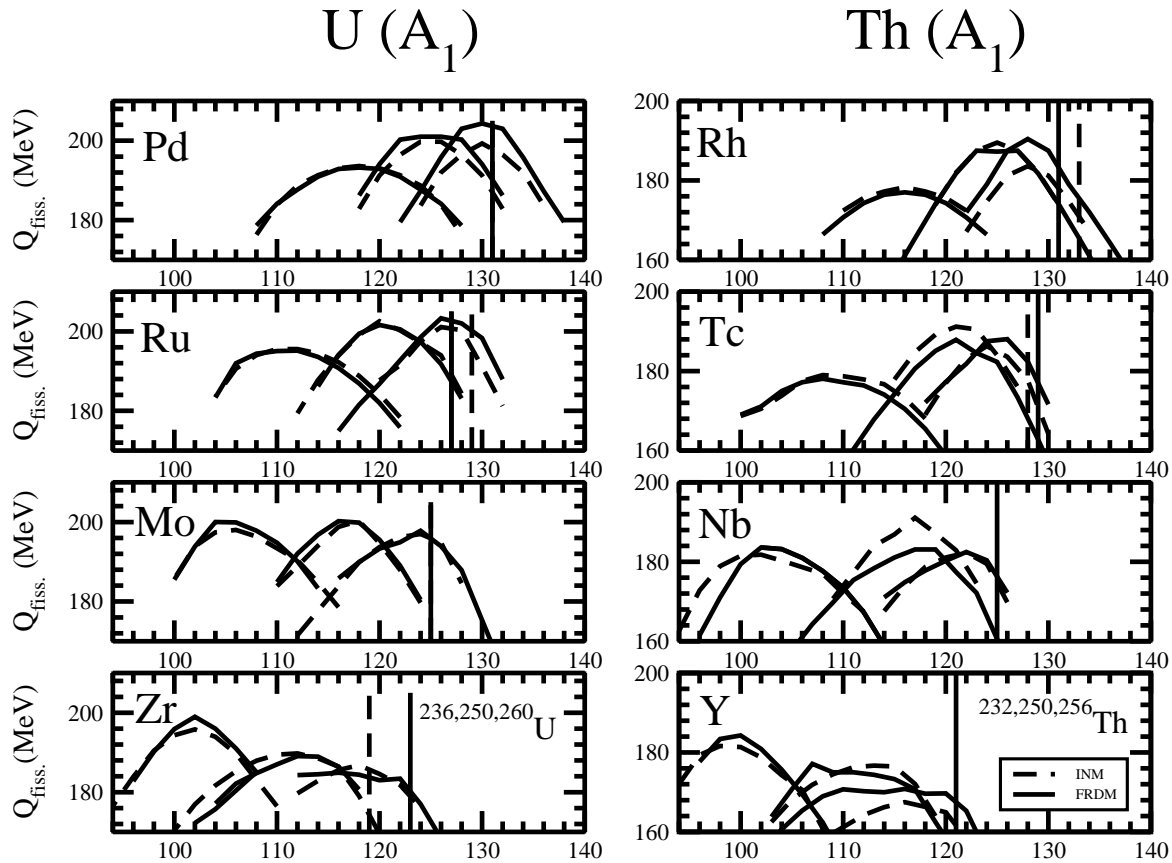


Figure 5. $Q_{fiss.}$ -value distribution given by $Q_{fiss.} = BE(A_1, Z_1) + BE(A_2, Z_2) - BE(A, Z)$ for $^{236,250,260}\text{U}$ and $^{232,250,256}\text{Th}$ as a function of A_1 fragment in the binary decay $A \rightarrow A_1 + A_2$. The binding energy used for calculation of Q -value is taken from [28] and Refs. [32] for FRDM and INM, respectively. The fission yield decreases drastically with increase or decrease of mass number of given element. Therefore, we have shown the distribution in the range 90 to 100% of the peak value in each case. The vertical line marks the neutron drip-line for the corresponding element in each panel. The full and dashed line denote the calculations with FRDM and INM mass models respectively.

References

- [1] Bonneau L and Quentin P, 2005 *Phys. Rev.* **C72** 014311.
- [2] Dubray N, Goutte H and Delaroche J -P 2008 *Phys. Rev.* **C77** 014310.
- [3] Younes P and Gogny D 2009 *Phys. Rev.* **C80** 054313.
- [4] Staszczar A, Dobaczewski J and Nazarewicz W, 2005 *Int. J. Mod. Phys.* **E14** 395.
- [5] Negele J, Koonin F, Möller P, Nix J R and Sierk A J, 1978, *Phys. Rev.* **C17** 1098.
- [6] Villars F 1977, *Nucl. Phys.* **A285** 269; Barranger M and Venerony M, 1978 *Ann. Phys.* **114** 123; Goeke K and Reingard P G 1978, *Ann. Phys.* **112** 328; Mukherjee A K and Pal M K 1982, *Nucl. Phys.* **A373** 289.
- [7] Pal M K 1993, *Nucl. Phys.* **A** **556** 201.
- [8] Goutte H, Berger J F, Casoli P and Gogny D 2005 *Phys. Rev.* **C71** 024316.
- [9] Ichikawa T, Iwamoto A and Möller P 2009 *Phys. Rev.* **C79** 014305.
- [10] Möller P, Madland D G, Sierk A J, Iwamoto A 2001 *Nature* **409** 785.
- [11] Gherghescu R A, Poenaru D N and Carjan N 2008 *Phys. Rev.* **C77** 044607.

- [12] Carjan N , Talou P and Serot O 2007 Nucl. Phys. **A792** 102.
- [13] Madler P 1985, Z. Phys. **A321** 343.
- [14] Samanta M S, Anand R P, Choudhury R K, Kooper S S, Nadkarni D M 1995 Phys. Rev. **C51** 3127.
- [15] Thoennessen N, 2004 Rep. Prog. Phys. **67** 1187.
- [16] Satpathy L, Patra S K and Chouthury R K 2008 *PRAMANA J. Phys.* **70** 87.
- [17] Walecka J D, 1974 Ann. Phys. (N.Y.) **83** 491.
- [18] Serot B D and Walecka J D, 1986 Adv. Nucl. Phys. **16** 1.
- [19] Boguta J and Bodmer A R 1977 Nucl. Phys. **A292** 413.
- [20] Lalazissis G A, König J and Ring P, 1997 Phys. Rev. **C55** 540; Sharma M M, Farhan A R and Mythili S 2000 Phys. Rev. **C61** 054306.
- [21] Patra S K, Bhat F H, Panda R N, Arumugam P, Gupta R K 2009 Phys. Rev. **C79** 044303.
- [22] Flocard H, Quentin P and Vautherin D 1973 Phys. Lett. **B46** 304.
- [23] Koepf W and Ring P 1988 Phys. Lett. **B212** 397.
- [24] Fink J, Blum V, Reinhard P -G, Maruhn J A and Greiner W 1989 Phys. Lett. **B218** 277.
- [25] Raman S, Nestor C W, and Tikkanen P, 2001 At. Data and Nucl. Data Tables **78** 1.
- [26] Audi G, Wapstra A H, and Thibault C 2003 Nucl. Phys. **A729** 337.
- [27] Angeli I, 2004 At. Data and Nucl. Data Tables **87** 185.
- [28] Möller P, Nix J R, Myers W D and Swiatecki W J 1995 At. Data and Nucl. Data Tables, **59** 185; Möller P, Nix J R and Kratz K -L 1997 At. Data and Nucl. Data Tables, **66** 131.
- [29] Bonneau L, 2006 Phys. Rev. **C74** 014301.
- [30] Arumugam P, Sharma B K, and Patra S K and Raj K Gupta 2005 Phy. Rev. **C71** 064308.
- [31] Brink D M, Int. School of Physics, Enrico Fermi, Course 36 (academic press 1966).
- [32] Nayak R C and Satpathy L 1999 At. Data and Nucl. Data Tables, **73** (1999).
- [33] Satpathy L, Uma Maheswari V S and Nayak R C 1999 Phys. Rep. **319** 85.
- [34] Satpathy L and Nayak R C 1998 J. Phys. **G24** 1527.